Evaluation of Alternative Power Production Efficiency Metrics for Offshore Wind Turbines and Farms

Briana Niu[a], Hoon Hwangbo[b], Li Zeng[b], Yu Ding[b,*]

[a] *Industrial Engineering and Operations Research Department, University of California, Berkeley, CA 94720, USA*

[b] *Department of Industrial and Systems Engineering, Texas A&M University, College Station, TX 77843, USA*

Abstract

The use of power production efficiency metrics for wind turbines is important for evaluating their productivity and quantifying the effectiveness of actions that are meant to improve the energy production. The goal of this research is not to propose a new efficiency metric since there are already multiple efficiency metrics widely used in practice: availability, power generation ratio, and power coefficient. Our objective here is to sort out the question of how these efficiency metrics are related to, or different from, one another. We believe addressing this research question has a great degree of practical significance as it is a question practitioners are often puzzled with. Understanding the similarities and differences of multiple efficiency metrics may even lay a foundation for the future proposals of new efficiency metrics. Our evaluation of whether the existing metrics are consistent with each other is driven by the use of actual data from an offshore wind farm. We observe that the three metrics show some degree of consistency but the power generation ratio, albeit the least popular, appears more representative of all metrics and more illustrative of the underlying efficiency. We also found that there is about 4% efficiency difference between wake-free and in-the-wake turbines for this specific wind farm.

Keywords: availability, power coefficient, power generation ratio, turbine performance, wake effect, wind farm operations

*Corresponding author. Tel.: +1 979 458 2343
Email address: yuding@tamu.edu (Yu Ding)

1. Introduction

Wind energy is a sector of renewable energy production that relies on capturing energy from the wind. The wind, the source of this energy, is highly stochastic and intermittent, so maintaining the efficiency of the energy production at a satisfactory level is critical for its broader usage as a power supply. The efficiency of the energy production can be improved by effective operational controls [1], condition monitoring and preventive maintenance [2], and/or timely upgrade and replacement of turbine components [3]. A well-defined efficiency metric, therefore, not only provides a better overview of how efficiently a turbine is running but also supports various decision-making processes regarding the operations and maintenance (O&M) of wind turbines and farms by quantifying the impact and effectiveness of an action that had been performed or is to be performed.

Various types of efficiency metrics for wind turbines and farms are available in literature. Depending on context, one may distinguish between turbine efficiency, generator efficiency, and transmission and storage efficiency [4], between aerodynamic efficiency, transmission efficiency, and conversion efficiency [5], or between power extraction efficiency and power generation efficiency [6]. To make it clear, in this paper, we focus on wind power production efficiency—how well a turbine, as a holistic system, produces power output given wind resources. We refer to this power production efficiency simply as efficiency throughout this paper.

Quantifying the efficiency of wind power production is a challenging task as the power production involves sophisticated aerodynamics and multiple factors, with some of them unknown or unobservable, affecting the efficiency. Currently, the industry standard, under IEC 61400-12-1, recommends using power coefficient [7] established upon significant simplification of the complicated nature of the power production system. Such simplification sometimes renders the metric inadequate for a proper representation of the efficiency of wind turbines in operation. Due to these challenges in efficiency quantification, it is common in practice to use multiple metrics for evaluating the efficiency of wind turbines and farms [8].

When evaluating the efficiency based on multiple metrics, an immediate question to be addressed is whether or not the evaluation from each metric draws the same conclusion. In this paper, we consider three metrics that are most commonly used in practice, namely, availability, power generation ratio, and power coefficient, and aim to address the aforementioned question. If the metrics do not always agree with one another (they indeed do not), then subsequent questions are how consistent the results based on the different metrics are and which metric provides better insight concerning the efficiency of turbines and farms. We try to answer these questions and make suggestions accordingly.

Other than the three efficiency metrics stated above, there are more complicated efficiency metrics emerging in the literature, for example, the new metric recently introduced in [9]. Although the efficiency metric proposed in [9] is more advanced and may gain popularity in the long run, it is not yet widely used as the aforementioned three metrics and its computation is much more involved. We decide to exclude this new metric for the comparison in this paper. On the other hand, the metric in [9] is calculated based on power curves (as the fraction of average power curve over full potential power curve), so it is similar to power generation ratio in nature. The insight garnered for the power generation ratio could be possibly used to shed lights on the relationship between the metric in [9] and others.

We would like to stress that the goal of this research is not to propose a new efficiency metric, but instead, it is to address the question of how the existing metrics are related to, or different from, one another. We believe addressing this research question is sufficiently meaningful, as keeping adding new efficiency metrics without thoroughly understanding the existing ones tends to confuse the practitioners, rather than helps clarify the matter. Understanding the similarities and differences of the existing efficiency metrics may in fact lay the foundation for the future proposals of new efficiency metrics.

The task of evaluating the alternative efficiency metrics is not trivial, primarily because there is no universal criterion determining the consistency of the metrics. In addition, the intrinsic efficiency of turbine itself is not directly observable nor is the underlying truth known, so it is difficult to decide which metric is better and in what aspect. We compare and evaluate the three metrics concerning how they are related to one another by using a set of tools of probability distribution, pairwise difference, correlation and linearity. As the metrics are defined over a given time duration, the analysis results may depend on the length of the time duration. We consider different time resolutions in analysis to address this issue.

The subsequent sections proceed as follows. Section 2 presents the definitions of the three metrics and describes how to calculate them using turbine operational data. Section 3 examines the relations and differences of the calculated metrics at multiple time resolutions and determines if they are consistent with each other. We also analyze whether one metric is superior to the others if they are not always consistent. Based on the findings in Section 3, Section 4 applies the efficiency metric(s) to characterize the efficiency of an offshore wind farm with a special focus on the wake effect. Section 5 concludes the paper.

2. Common Efficiency Metrics for Wind Power Production

In this section, we describe three efficiency metrics for wind power production: availability, power generation ratio (PGR), and power coefficient. We also explain their calculation procedures.

Following the industry standard IEC 61400-12-1 [7], we use 10-minute averaged measurements for calculation of the metrics. Based on the IEC standard, wind speed is first adjusted by air density through

$$V = V' \left(\frac{\rho}{\rho_0}\right)^{1/3}, \tag{1}$$

where V' and V are the wind velocity measurements before and after the adjustment, respectively, ρ denotes air density calculated from the measurements of air pressure and air temperature, and $\rho_0 = 1.225\,\mathrm{kg/m^3}$ is the international standard atmosphere air density at sea level and $15\,^\circ\mathrm{C}$.

Suppose that we are interested in the efficiency of wind turbines measured for a specific time duration, which could be a week, a month, or a year. Consider a weekly resolution as an example. We then calculate efficiency metrics for every single week and evaluate the time series of the metrics with the unit time of a week. The same calculation can be easily extended to other time resolutions. Let (V_t, ρ_t, P_t) for $t = 1, \ldots, T$ denote a data pair observed during a given time period (a week for weekly resolution), where P represents the power output measurements and T is the total number of the data pairs observed during the time period. We calculate a single value of an efficiency metric for each given time period using (V_t, ρ_t, P_t) for $\forall t = 1, \ldots, T$.

2.1. Availability

One of the efficiency metrics used broadly in the wind industry is availability [10, 11] described in the industry standard IEC TS 61400-26-1 [12]. The availability tracks the amount of time in which power is produced by a turbine and then compares it to the total amount of time for which the turbine could have produced power. A wind turbine is supposed to produce power when the wind speed is between the cut-in and cut-out wind speeds, which are the design characteristics of a given turbine. The cut-in speed is the minimum wind speed needed for the turbine to begin operating and generating power. The cut-out speed is the point at which the wind speed reaches its maximum level allowed for safe operation of the turbine. At this speed, the blades are braked and feathered to stop operation, preventing the turbine from damages that may be caused by a harsh wind condition [13]. Turbines are expected to produce power at all times when recorded wind speeds are within these two limits. If a turbine does not produce power when the wind conditions are allowing, the turbine is then deemed unavailable. The availability is thus defined as

$$\text{Availability} = \frac{\#\{(V_t, \rho_t, P_t):\ P_t > 0,\, V_{ci} \le V_t \le V_{co},\, t = 1, \ldots, T\}}{\#\{(V_t, \rho_t, P_t):\ V_{ci} \le V_t \le V_{co},\, t = 1, \ldots, T\}}, \tag{2}$$

where $\#\{\cdot\}$ counts the number of elements in the set defined by the brackets, and V_{ci} and V_{co}, respectively, are the cut-in and cut-out wind speeds. The denominator in (2) approximates the total time (in terms of the number of 10-min intervals) that a turbine is expected to produce power [14], whereas the numerator approximates the total time that a turbine does produce power.

2.2. Power generation ratio

While the availability calculates a ratio in terms of the amount of up running time, PGR defines a ratio relevant to the amount of power output. The idea is similar to that of *production-based availability*, recently advocated by the industry standard IEC TS 61400-26-2 [15]. By contrast, the availability discussed in the preceding section is referred to as *time-based availability*. The production-based availability calculates the ratio of actual energy production to potential energy production, where the potential energy production is the sum of actual energy production and lost production that is caused by an abnormal operational status of a turbine (e.g., downtime, curtailment). The lost production needs to be estimated and its estimation requires detailed information about a turbine's operating status, not easily accessible to anyone outside the immediate operator of a wind turbine or wind farm.

Instead of estimating the lost production, we make a revision in this paper, making the assessment easier to carry out. Our revision is to use a

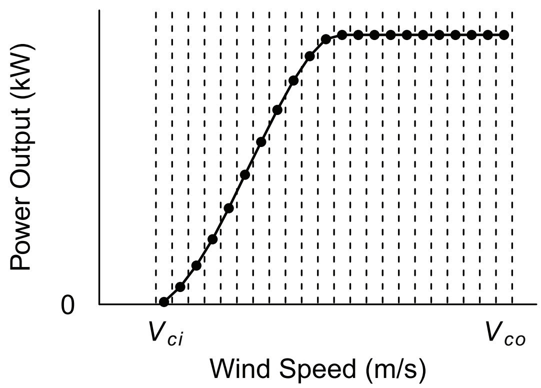

Figure 1: Manufacturer's power curve. The dots indicate the power curve estimates evaluated at each bin, and the piecewise linear curve connecting all the dots forms the nominal power curve. The dashed vertical lines illustrate the wind speed bins.

nominal power curve provided by a turbine's manufacturer for calculating the value of potential energy production. The resulting ratio is in fact the PGR mentioned earlier, which is in spirit similar to the production-based availability.

A power curve defines power output as a function of wind speed and estimates power output for a given wind speed. As such, the potential energy production in the PGR can be written as $\hat{P}(V_t)$ for given V_t where the function $\hat{P}(\cdot)$ denotes a nominal power curve. Then, the PGR of a given time duration (including T observations) can be computed as

$$\mathrm{PGR} = \frac{\sum_{t=1}^{T} P_t}{\sum_{t=1}^{T} \hat{P}(V_t)}. \tag{3}$$

IEC recommends that the nominal power curve be estimated by the method of binning [7]; see Figure 1. The method first generates multiple bins with equal size (e.g., 1 m/s) partitioning the domain of wind speed. For each bin, the sample mean of power output is calculated from the power data whose wind speed falls into the specific bin. The sample mean together with the middle point of the bin provide a point-wise estimate of the power curve evaluated at the middle point of the bin. Connecting these estimates derives a piece-wise linear curve defining the nominal power curve. A nominal power cure, in terms of the point-wise estimates, is usually provided by the turbine's manufacturer.

2.3. Power coefficient

Different from the availability and PGR, power coefficient explicitly reflects a law of physics, and it measures the aerodynamic efficiency of a wind turbine. Power coefficient (C_p) refers to the ratio of actual energy production to the energy available in the ambient wind flowing into the turbine blades [16]. The available energy in the wind can be characterized by air density, turbine's blade swept area (A), and wind velocity. As such, C_p is calculated as

$$C_p(t) = \frac{2P_t}{\rho_t A V_t'^3}, \tag{4}$$

for any given observation t. Note here that the C_p calculation uses the wind speed V' (without air density adjustment) since the calculation itself involves air density.

For a given time period (say, a week), there are multiple C_p values; in fact, T of them in total. The C_p values can be plotted against the wind speed. Then, one can bin the C_p values by groups of 1 m/s according to their respective wind speeds and get the averages of C_p for individual bins. By doing so, a C_p curve is produced, in a similar fashion as how the nominal power curve is produced. The maximum value on the C_p curve is chosen as the turbine's representative power coefficient [9, 17]. Hereafter, we refer to this peak value on a power coefficient curve as the power coefficient unless otherwise stated.

3. Comparison of the Metrics

We compare the metrics described in the previous section by using actual operational data provided by an offshore wind farm. Table 1 and Figure 2 present some information about the wind farm and a rough sketch of the wind farm's layout, respectively.

The dataset was produced over a span of four years ranging from 2007 to 2010. It includes measurements which were recorded at each individual turbine as well as other atmospheric statistics that were tracked by a meteorological mast. We extract the data needed for the calculation of the metrics and match the data points for a turbine and the mast by aligning their respective timestamps. After such an alignment, any time point with missing data are eliminated.

Temporal resolutions to be examined include weekly, monthly, quarterly, and yearly time resolutions with a primary focus on weekly and monthly as

Table 1: Information about the offshore wind farm. The d in the last two rows refers to rotor diameter. NW-SE and NE-SW denote northwest-southeast orientation and northeast-southwest orientation, respectively. Values are given in a range or as an approximation, due to a confidentiality agreement in place forbidding the disclosure of the exact corresponding values.

Location	Europe
Number of wind turbines	30–40
Cut-in wind speed (m/s)	3.5
Cut-out wind speed (m/s)	25
Rated wind speed (m/s)	approximately 15
Rated power (MW)	approximately 3
Turbine spacing: NW-SE	7–8d
Turbine spacing: NE-SW	11–12d

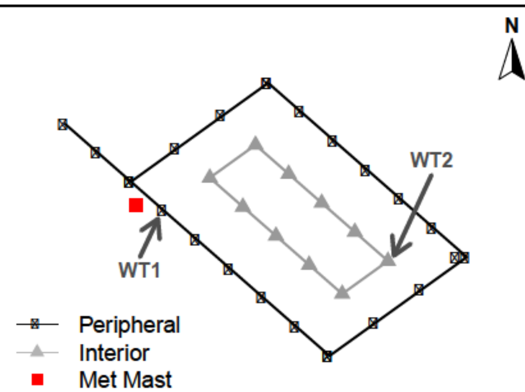

Figure 2: A rough sketch of the layout of the offshore wind farm. This wind farm has 30–40 turbines with 20–26 peripheral turbines and 10–15 interior turbines. Peripheral turbines are located along the black lines and interior turbines along the gray lines. A meteorological mast is indicated by a square near the left edge of the farm.

they provide greater amounts of data points and detail. Quarterly and yearly resolutions are used for more general trends and comparisons.

For each temporal resolution, we calculate the three metrics of availability, PGR, and power coefficient as described in Section 2; hereafter denoted as M1, M2, and M3, respectively. While the averages of M1 and those of M2 calculated for each turbine are within a similar range (0.75–1), the averages of M3 are noticeably lower at the 0.35–0.5 range, about half the values of M1 and M2. This is understandable as power coefficient (M3) is limited by the Betz Limit to a theoretical maximum of 0.593, though a commercial turbine realistically operates at about 0.45 [18]. To make all the three metrics comparable in magnitude, we multiply M3 by two and use the rescaled metric (2×M3) for the subsequent analysis.

We first plot the time-series of the three metrics for a peripheral turbine that locates the closest to the met mast (referred to as WT1 hereafter). Figure 3(a) presents the time-series of the metrics generated based on the monthly resolution over the four-year span. The figure demonstrates that the metrics follow similar overall trends, with peaks and troughs at similar periods of time. The level of variation associated with the three metrics looks similar. In fact, all the three metrics have similar coefficients of variation, though the one for M2 tends to be slightly higher—on average, 0.264 for M2 compared to 0.254 and 0.252 for M1 and 2×M3, respectively. These patterns and characteristics are consistently observed in the other turbines on the wind farm. The similar insights can be drawn for the weekly resolution.

In Table 2, we calculate correlation coefficients between the metrics for WT1. Similar to the first two rows of the table, the correlation coefficients are above 0.9 for all turbines, indicating strong correlations between the metrics. By considering the well-aligned time-series and the high correlation coefficients, one may impetuously conclude that the three metrics are consistent with each other and they can substitute for each other when evaluating the efficiency of turbines. However, if we eliminate some periods of nearly zero power production (for example, a period for which any metric is below 0.2;

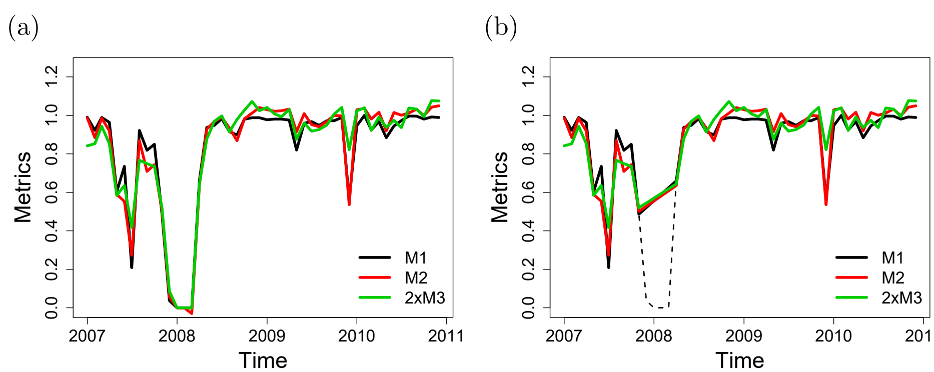

Figure 3: All three metrics plotted at monthly time resolution for WT1: (a) for the full period; (b) after eliminating the periods in which the turbine does not operate for most of the time (dashed line).

Table 2: Correlation between metrics for WT1. Weekly and monthly temporal resolutions are shown.

	M1 & M2	M1 & 2×M3	M2 & 2×M3
Weekly resolution (full)	0.975	0.946	0.959
Monthly resolution (full)	0.986	0.966	0.978
Weekly resolution (reduced)	0.843	0.661	0.785
Monthly resolution (reduced)	0.956	0.876	0.929

see Figure 3(b)), which may be due to pitch system faults [19], gear box faults [20], or some scheduled maintenance, or a combination of these reasons, the metrics based on such a reduced period produce significantly lower correlation coefficients—for this particular turbine, as low as 0.661 between M1 and 2×M3 at weekly time resolution. This implies that the original high correlation derived from the full period data could be contributed substantially by the non-operating periods of the turbine, which further suggests possible disparity between the metrics under typical operating conditions.

In the following sections, we use the metric values calculated for the reduced period only, in order to better differentiate the metrics in terms of their capability of quantifying the efficiency of turbines.

3.1. Distributions

Figure 4 demonstrates the distributions of the calculated metrics for a single turbine, but it is representative of the other turbines as they all show similar distribution spreads. While M2 and 2×M3 both have relatively broad spreads of data, M1 has a much narrower range. A significant portion of its density is concentrated near one at which the distribution is truncated, with a steep taper to lower values. In contrast, M2 and 2×M3 both take the shape similar to the bell-shaped curve with smoother tapers in both directions. M1's concentration of values makes it difficult to differentiate between the efficiency of turbine at different time periods. As more values are within the same range, the variations in turbine performance are concealed. This can potentially mislead turbine operators into believing that the turbines operate at a similar efficiency level, even though the underlying turbines' efficiency levels differ.

Such a unique distributional characteristic of M1 can be inferred by its calculation procedure. As expressed in Eq. (2), the numerator of M1 counts

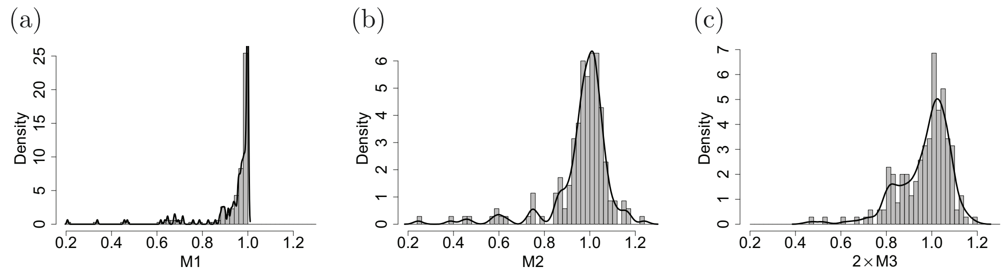

Figure 4: Probability densities of the metric values at weekly time resolution for WT1: (a) M1; (b) M2; (c) 2×M3.

the number of members in a set that is a subset of the one associated with the denominator, so it has a maximum value of one at all points in time. This is a desired property for an efficiency metric, which is not observed from M2 or 2×M3. M2 can exceed one because manufacturers' power curves display expected power values as an averaged measure and particular instances of power production may exceed the expected productions [21]. The value of 2×M3 is bounded from above by the Betz Limit at 1.186 (after rescaling), which itself is greater than one. It is interesting to observe that M2 appears to be bounded by a value similar to 1.186.

The unique property of M1 when combined with its binary quantification of whether or not power was generated, however, adversely affects its quantification capability. As long as a turbine is generating power at a point in time, that point would be counted as a one. Even some time points with power production that is significantly lower than expected would still be counted as ones. Averaging over these counts produces the metric weighted heavily towards one. Periods with high efficiency (in terms of the amount of actual power production) look the same as low efficiency periods as long as the power produced exceeds a low threshold.

The methods calculating M2 and M3, on the other hand, allow for a sliding scale measure of power production so that they account for how much power was produced. Values of M2 and 2×M3 thus have greater spread and do not concentrate as narrowly around any particular value as M1 does. This ability to better distinguish between time periods of differing performance as well as the distributional features render M2 and 2×M3 stronger metrics than M1. They allow for a more detailed portrayal of a turbine's efficiency over time as opposed to M1's more general overview of whether or not the turbine was in operation.

3.2. Pairwise differences

Figure 5 illustrates the absolute difference between the calculated metrics on a weekly basis. Darker bars indicate the periods of significantly large differences while lighter bars are for the periods of smaller differences.

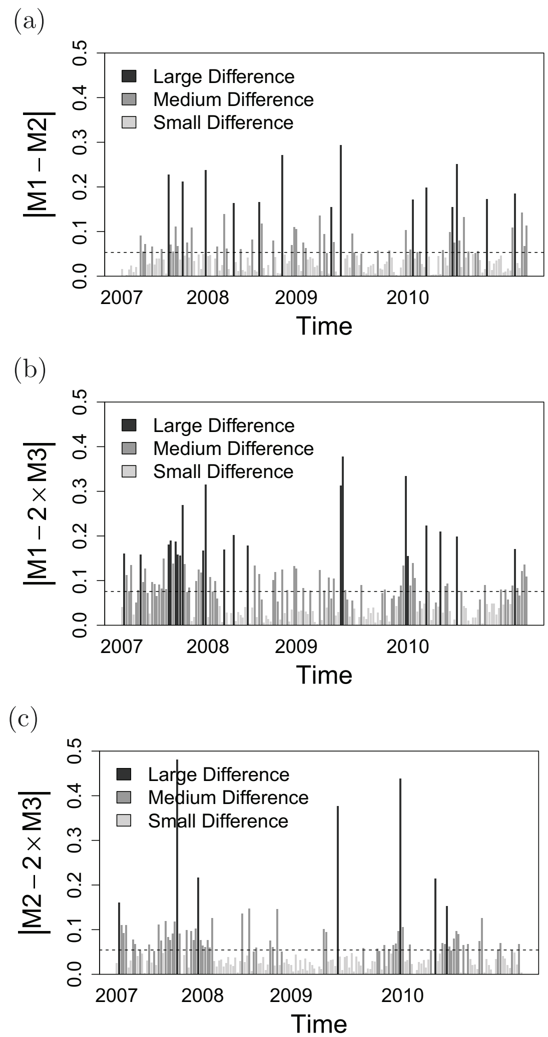

Figure 5: Magnitudes of absolute difference between metric values at weekly resolution for WT1: (a) M1 vs M2; (b) M1 vs 2×M3; (c) M2 vs 2×M3. The dashed line in each plot is the average of the absolute differences in that plot. An absolute difference is considered as a small difference, if its value is smaller than 0.05, as a large difference, if its value is greater than 0.15, and as a medium difference, if its value is in between.

Figure 5(c) shows that the large differences between M2 and 2×M3 are sparsely distributed through the four years. In contrast, as shown in Figure 5(a) and Figure 5(b), there are significantly more instances of large value differences between M1 and either of the other metrics, especially between M1 and 2×M3. This implies that both M1 and 2×M3 are more similar to M2 than to each other. M1 and M2 calculate a ratio of the actual performance over the expected performance, although M1 focuses on the amount of time and M2 examines the amount of power. This sets 2×M3 apart from M1 and M2. On the other hand, M2 and 2×M3 quantify the efficiency of turbine with respect to the amount of power production, whereas M1 concerns the amount of operational time, which makes M1 distinct from the other two.

In Figure 5, the large or medium differences tend to be heavily concentrated within some specific periods, notably in the second half of 2007 and the first half of 2010. In fact, these periods represent those in which turbines' true efficiencies are relatively low. There are two different aspects describing this phenomenon.

First, recall from Figure 4 that M1 tends to be heavily weighted towards its maximum, overestimating turbine's efficiency in the relative scale. If a turbine produced some power for most time instances within a given period, its availability should be close to one. The large differences between M1 and the other two metrics then imply that the turbine was producing some power for most of the times but the amount of the power production was considerably low relative to its expectation (in Figure 3, see the later part of 2007 where M1 is higher than the other two).

Secondly, recall that M3 represents a *maximum effect* (on the C_p curve), whereas M2 is an *integration effect*. For a functional response, the two effects can be understandably different. The large differences between M2 and 2×M3 suggest that a turbine produced a sufficient amount of power only for a small portion of the given time period. In this case, the turbine's maximum efficiency measured by 2×M3 is relatively high, but M2 is relatively low because the turbine did not produce much power on average during the same period (see the middle of 2007 and the beginning of 2010 in Figure 3). M1 also measures an *integration effect*, but in terms of the operational time, so the same argument is applicable when explaining the difference between M1 and 2×M3. Most of the time, when there is a large difference between M2 and 2×M3, a large difference between M1 and 2×M3 is also observed (see Figure 5(b) and 5(c)).

All of these observations can be found in the cases of other turbines as well. Although the concentration periods of large and medium differences vary, all turbines display the clustering pattern, and such clusters are closely related to the different characteristics of the metrics.

When comparing the mean of the absolute differences between the metrics (indicated by the dashed horizontal lines in Figure 5), the disparity between the metrics becomes less pronounced. While a metric pair with the smallest mean difference varies by turbines, the largest mean difference is consistently observed between M1 and 2×M3, sometimes by a significant amount than that between M1 and M2 or M2 and 2×M3. This suggests that M2 has comparably closer values to M1 and 2×M3. As such, M2 is more consistent in value with either of M1 and 2×M3 and its values are a better reflection of all the three metrics.

3.3. Correlations and linear relationships

As shown in Table 2, we calculate correlation coefficients between the metrics based on the reduced data set (periods of nearly zero power production removed). The post-removal correlation is the highest between M1 and M2 for most turbines. The correlations between M2 and 2×M3 (or equivalently, between M2 and M3) are also relatively high. For most turbines, the correlation coefficients between M1 and M2 remain within the 0.8 range at weekly resolution while those between M2 and M3 are generally in the 0.7 range.

The lowest correlations are found between M1 and M3 for all turbines and time resolutions, with the correlation coefficient values usually around 0.5–0.6 but dipping sometimes into the 0.4 range. The values displayed in Table 2 are among the higher values of M1-M3 correlation of turbines. Another turbine has an M1-M3 correlation of just 0.417 for the reduced weekly data. This indicates that the relationship between these two metrics is much weaker, highlighting the strength of M2 for its much stronger relationship with either of the other metrics.

Weekly time resolution is best for highlighting difference in correlation between metrics. Correlations rise as the time resolution becomes coarse; monthly, quarterly, and yearly resolutions in general return a correlation in the range of 0.9. We believe that the averaging effect when using a coarse time resolution irons out a certain degree of details, making the metrics based on the coarse time resolutions less differentiating.

To analyze the consistency of the metrics, we also evaluate the linearity between any pair of the metrics around $y = x$ line. Suppose that we generate data points (x, y) paired by the values of two metrics. If the data points perfectly fit to the $y = x$ line, an increase in one metric implies the same amount of increase in the other metric. As such, their ability to capture changes in efficiency is identical, or equivalently, they are consistent.

However, as noted earlier, the scales of the metrics are not the same, e.g., M1 and M2 are about twice of the unscaled M3. Assessing the extent of linearity around the $y = x$ line thus requires to match the scales between the metrics.

To align the scales, we perform linear regression upon the different metric pairs. For example, for the M1–M2 pair, we fit a linear model of M1 $= \beta \cdot$ M2 $+ \epsilon$ to estimate β, where ϵ is a random noise term. Let $\hat{\beta}$ denote the coefficient estimate. We then use the estimate $\hat{\beta}$ to rescale the values of M2, generating scale-adjusted data points (M1, $\hat{\beta}\cdot$M2). With the scale adjustment, the data points should be centered about the $y = x$ line. If they show strong linearity around the $y = x$ line, we can conclude the metrics for the corresponding pair are consistent with each other. To determine the extent of linearity, the average magnitude of the data points' vertical distance from the $y = x$ line (in an absolute value) is computed.

Figure 6 presents the scatter plots of the scale-adjusted metrics and the $y = x$ line. For the illustration purpose, we show the result of the peripheral turbine used so far (WT1) as well as the result of an interior turbine (WT2). For the metrics calculated for the peripheral turbine, the linear regression yields the scale adjustment coefficients ($\hat{\beta}$) of 0.97, 1.93, and 1.99 for M1–M2, M1–M3, and M2–M3 pairs, respectively. The coefficient of 0.97 for the M1–M2 pair, for instance, implies that M2 will have the same scale with M1 after multiplying it by 0.97. For the interior turbine, the scale adjustment coefficients are 0.98, 2.01, and 2.06, respectively.

In the figure, points are more concentrated near where x and y equal one. Whenever x refers to M1, there is a very apparent clustering of points at $x = 1$ due to the truncation of the distribution of M1 at one. On the other hand, the data points for the M2–M3 pair are well spread around the region, a characteristic reminiscent of the metrics' distributions examined earlier.

After the scale-adjustment, the data points tend to be placed above the $y = x$ line for relatively low x values, e.g., less than 0.8, whenever y-axis represents a rescaled M3 (triangles and diamonds). This confirms the difference between the maximum effect (for M3) and the integration effect (for M1 and M2) discussed earlier.

As shown in Table 3, the average distances between the points and the

(a)

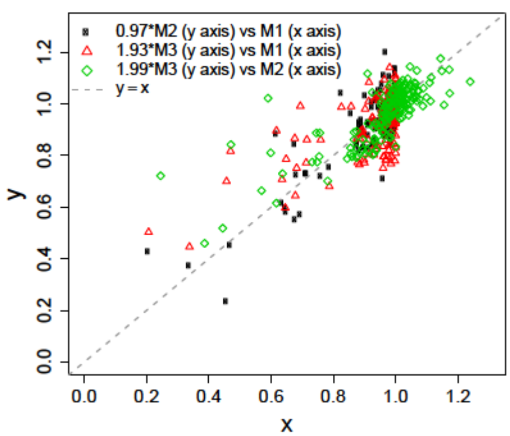

(b)

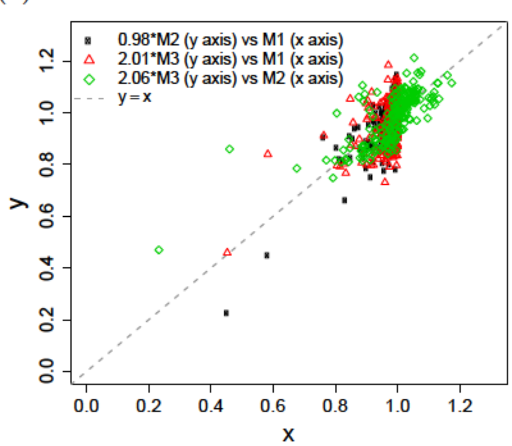

Figure 6: Linear relationships between metrics at weekly time resolution: (a) for a peripheral turbine WT1; (b) for an interior turbine WT2. Plots generated from scaling values by the x to y ratio. The dashed line illustrates $y = x$ line. The x and y axes vary for each relationship as defined in legend.

$y = x$ line is the greatest for the M1–M3 pair for both turbines, suggesting that the M1–M3 pair has the weakest extent of linearity. This reinforces the understanding from the analysis of absolute differences that M1 and M3 are the least consistent metrics, while M2 has stronger relationship with both other metrics.

Table 3: Average absolute vertical distances from the $y = x$ line.

	M1 vs $\hat{\beta}$·M2	M1 vs $\hat{\beta}$·M3	M2 vs $\hat{\beta}$·M3
A peripheral turbine	0.050	0.068	0.055
An interior turbine	0.046	0.068	0.052

3.4. Overall insight

According to the above analyses, while all metrics display some level of consistency, M2 is the most consistent with the other metrics. The absolute differences in metric values demonstrate that M2 produces values that are more representative of the three metrics. Correlations between the metrics also suggest that changes in turbine performance mapped by M2 are illustrative of such trends displayed by other metrics. Moreover, the evaluation of the linearity between the metrics shows that M1 or M3 has a stronger relation with M2 than with each other. It is not too far fetched to reach the conclusion that M2 better represents all three metrics.

Various aspects of our analysis have shown M1's deficiency in discriminating changes in turbine performance. Practitioners are well aware of M1's deficiency, which becomes the chief reason to recently adopt the production-based availability metric. The deficiency of M3 could sometimes be overlooked, and we hereby would like to re-iterate. M3 takes the maximum on a C_p curve. This maximum does not always effectively reflect turbine performance as it ignores the performance under some wind conditions that do not associate with the maximum point. A recent work indeed demonstrates this shortcoming of M3 by using a set of simulated data [9].

4. Evaluation of Wake Effect

Depending on the location of a turbine and where the wind comes from, a wind turbine may suffer from a significant amount of power loss due to wind velocity deficit and turbulence caused by the operation of nearby turbines; known as the wake effect [22]. Understanding the wake effect is important for maintaining the power production efficiency of a wind farm via effective operational controls [23, 24] and designing the layout of a wind farm in preparation [25, 26]. In this section, we analyze the wake effect and its influence on the power production efficiency by using the PGR (M2) to show the actual use of the metric in practice.

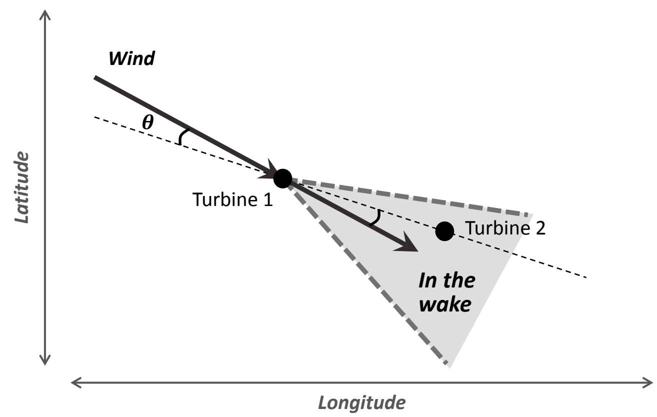

Figure 7: Range of angles for which the wake of Turbine 1 (upstream turbine) causes velocity deficit and hence power deficit if a turbine is within the range.

Figure 7 presents a snapshot of a wake situation (for illustration purpose only). The incoming wind loses its energy after being extracted by an operating turbine (Turbine 1), and this energy loss is revealed by velocity deficit at downstream locations. The level of the velocity deficit varies depending on the distance from the upstream turbine and the angle deviating from the wind direction (θ). The velocity deficit remains observable up to a certain angular deviation from the given wind direction. If another wind turbine (Turbine 2) is within this "in the wake" region (where the velocity deficit is expected; the shaded area), it experiences power deficit as a consequence of the velocity deficit. Given the fixed locations of the turbines, whether to expect a power deficit and how much deficit to expect strongly depends on where the wind comes from. When the wind direction reverses, the role of upstream and downstream will reverse, too.

To assess the loss in power production efficiency caused by wake effect, we first need to identify which turbines are free of the wake and which are in the wake, so that we can compare the power production efficiency between the two sets of turbines. Since the members of the two sets keep changing as wind direction changes, we partition the support of the direction into multiple wind sectors in each of which the two sets can be determined with confidence (see Figure 8). Algorithm 1 describes how we generated the wind sectors.

The basic idea of Algorithm 1 is that, to be a wake free turbine, the target turbine should not be in the wake region of a nearby turbine. Two

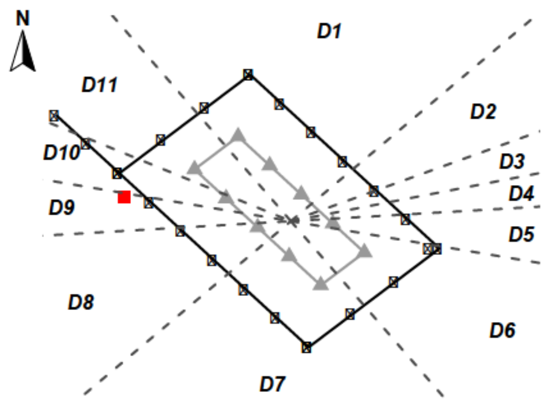

Figure 8: Multiple wind sectors. In each sector, the set of wake free turbines versus the set of turbines in the wake can be confidently determined based on the wind direction and wind power output data. Some sectors (D2–D4 and D10–D11) are narrower than others due to the irregular shape of the wind farm at the north-western corner.

Algorithm 1: Wind sector generation

Set the index of wind sector, s, to 1;
Fix wind direction D to a fixed number, for example, $D = 0°$;
Define the set of all turbines, $\mathcal{W}$;
Define the set of all peripheral turbines, $\mathcal{P}$;
repeat
    Initialize the set of wake free turbines $\mathcal{F}(s) \leftarrow \mathcal{P}$;
    for *each* $p \in \mathcal{P}$ **do**
        Calculate a pairwise distance between the turbine p and any other turbine $w \in \mathcal{W}$; denote it as $dist(w)$;
        Calculate $\theta(w)$, an acute angle between wind direction and the direction of a turbine $w \in \mathcal{W}$ relative to the turbine p (known as bearing);
        Remove p from $\mathcal{F}(s)$ if there is any w such that $dist(w) \leq 20d$ <u>and</u> $|\theta(w)| \leq 22.5°$;
    end
    Increase D until there is no change of $\mathcal{F}(s)$;
    Increase s by 1;
until D *reaches its initial value, i.e.,* $D = 0°$*, or equivalently,* $D = 360°$;

Table 4: Descriptive statistics of the group PGR calculated at weekly time resolution.

	Mean	25% quantile	Median	75% quantile	Standard Deviation
PGR_{itw}	0.987	0.932	0.965	1.001	0.113
PGR_{wf}	1.031	0.985	1.004	1.046	0.081

parameters are used to decide the wake region: the distance between two turbines and the wake angle. The distance threshold is chosen to be $20d$, where d is the rotor diameter, and the wake angle threshold is chosen to be $\pm 22.5°$ ($45°$ in total) [27, 28]. We consider only peripheral turbines as the candidates for a wake free turbine. Once the set of wake free turbines for a wind sector s, $\mathcal{F}(s)$, is determined, the set of turbines in the wake, $\mathcal{I}(s)$, is taken simply as the complementary set.

The wind sector generation additionally requires the information of wind direction. As such, we now use the data pairs $(V_t, D_t, \rho_t, P_{ti})$ for $t = 1, \ldots, T$ and $i = 1, \ldots, n$ where D_t denotes wind direction and i is an index for n turbines. Different from the previous analysis in Section 3, we use mast measurements for the wind speed V to account for the available wind resource that is common in the local area. The measurements are still 10-min based, and we use the weekly time resolution considering its effectiveness shown in Section 3.

To compare the wake-free turbines with the in-the-wake turbines, we calculate the PGR for each group. Let $\mathcal{J}_{wf}(D_t)$ and $\mathcal{J}_{itw}(D_t)$, respectively, denote the set of wake-free turbines and the set of in-the-wake turbines varying with wind direction at each time t. Then, we calculate the group PGR as follows

$$\text{PGR}_{wf} = \frac{\sum_{t=1}^{T} \sum_{i \in \mathcal{J}_{wf}(D_t)} P_{ti}}{\sum_{t=1}^{T} \sum_{i \in \mathcal{J}_{wf}(D_t)} \hat{P}(V_t)}, \quad \text{PGR}_{itw} = \frac{\sum_{t=1}^{T} \sum_{i \in \mathcal{J}_{itw}(D_t)} P_{ti}}{\sum_{t=1}^{T} \sum_{i \in \mathcal{J}_{itw}(D_t)} \hat{P}(V_t)}. \tag{5}$$

Figure 9 and Table 4, respectively, present boxplots and descriptive statistics of the group performance. As expected, the wake-free turbines show a higher power production level, and the difference between PGR_{wf} and PGR_{itw} is in the range of 4.0–5.3%. In terms of the mean and median, the difference is 4.4% and 4.0%, respectively.

The magnitude of the efficiency loss ($\text{PGR}_{wf} - \text{PGR}_{itw}$) is relatively small compared to the 10% power loss estimate stated earlier [29], where the per-

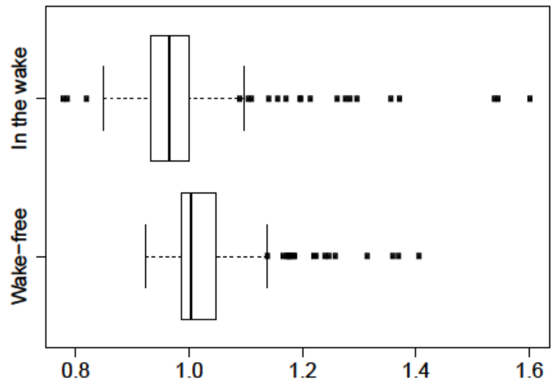

Figure 9: Boxplots of the group PGR calculated at weekly time resolution.

centage was calculated for an offshore wind farm comprising 20 turbines closely located in a row in a bow shape. For the wind farm studied in [29], the turbine spacing (between-turbine distance) is 2.4 times the rotor diameter (d), which is rather tight compared to typical turbine spacing. The offshore wind farm used in this study has the turbine spacing of approximately 7–8d and 11–12d for the northwest-southeast and northeast-southwest orientations, respectively. Considering the significant impact of turbine spacing on wake loss [28], it is not surprising to see the considerable gap between our result and the result reported in [29].

5. Concluding Remarks

In this paper, we examined the capabilities of different metrics for wind power production and compared three metrics broadly used in practice—availability, power generation ratio, and power coefficient. Power generation ratio was used as a proxy for the production-based availability, due to its easiness in computation. Nonetheless, power generation ratio itself can be used as a performance metric in practice, as illustrated in Section 4.

This study is important as it provides an answer to which metric among the three different kinds is the most accurate and reliable measure of turbine performance changing over time. We evaluated the three metrics in various aspects such as (i) probability distributions, (ii) pairwise differences, and (iii) correlations and linear relationships to determine how representative they are of the data as a whole.

Through our assessment, we found that power generation ratio is the strongest and most consistent metric for evaluating the offshore wind farm used in this study. The probability distributions of power generation ratio and power coefficient have relatively balanced tails on both sides of the mode, whereas the distribution of availability is truncated at a certain point and exhibits a small spread. In this aspect, power generation ratio and power coefficient are better metrics as their distributions allow for greater sensitivity to differences in the efficiency of turbine. When examining the pairwise absolute differences, the correlations, and the linear relationships between the metrics, we consistently found that the greatest dissimilarity existed between availability and power coefficient; on the other hand, power generation ratio was relatively well-matched with either of the other metrics. As power generation ratio was more representative of all three metrics, it could serve as the most comprehensive and reliable metric.

The analysis applied in this study was based on the data provided by a specific offshore wind farm. As such, we admit that the analysis results may not readily extend to other wind farms, although the procedure of analysis and examination is generalizable. Our experience indicates that the insights garnered here should also have good potential for generalization. Still, considering substantially different characteristics between onshore and offshore wind farms [30], extending this study to other wind farms, especially to onshore farms, would be interesting and useful while confirming whether the trends found in this study exist for farms in different environments.

Acknowledgments

Hwangbo and Ding's research was partially supported by the National Science Foundation under grants no. CMMI-1300560 and no. IIS-1741173. The authors also want to thank Mr. Víctor Gálvez Yanjarí, a visiting student from PUC, Chile, for helping with numerical analysis in Section 4.

References

[1] Abdullah MA, Yatim A, Tan C, Saidur R. A review of maximum power point tracking algorithms for wind energy systems. Renewable and Sustainable Energy Reviews 2012;16(5):3220–7.

[2] Pérez JMP, Márquez FPG, Tobias A, Papaelias M. Wind turbine reliability analysis. Renewable and Sustainable Energy Reviews 2013;23:463–72.

[3] Lee G, Ding Y, Xie L, Genton MG. A kernel plus method for quantifying wind turbine performance upgrades. Wind Energy 2015;18(7):1207–19.

[4] Roy S, Saha UK. Wind tunnel experiments of a newly developed two-bladed savonius-style wind turbine. Applied Energy 2015;137:117–25.

[5] Yang H, Lu L, Zhou W. A novel optimization sizing model for hybrid solar-wind power generation system. Solar energy 2007;81(1):76–84.

[6] de Prada Gil M, Gomis-Bellmunt O, Sumper A, Bergas-Jané J. Power generation efficiency analysis of offshore wind farms connected to a slpc (single large power converter) operated with variable frequencies considering wake effects. Energy 2012;37(1):455–68.

[7] International Electrotechnical Commission (IEC) . IEC 61400-12-1 Ed. 1, Wind turbines - part 12-1: power performance measurements of electricity producing wind turbines. Geneva, Switzerland: IEC; 2005.

[8] Lydia M, Kumar SS, Selvakumar AI, Kumar GEP. A comprehensive review on wind turbine power curve modeling techniques. Renewable and Sustainable Energy Reviews 2014;30:452–60.

[9] Hwangbo H, Johnson A, Ding Y. A production economics analysis for quantifying the efficiency of wind turbines. Wind Energy 2017;20(9):1501–13.

[10] Conroy N, Deane J, Gallachóir BPÓ. Wind turbine availability: should it be time or energy based?—a case study in ireland. Renewable Energy 2011;36(11):2967–71.

[11] Tavner P, Faulstich S, Hahn B, van Bussel G. Reliability & availability of wind turbine electrical & electronic components. EPE Journal 2010;20(4):45–50.

[12] International Electrotechnical Commission (IEC) . IEC TS 61400-26-1 Ed. 1, Wind turbines - part 26-1: time-based availability for wind turbine generating systems. IEC; 2011.

[13] Stankovic S, Campbell N, Harries A. Urban wind energy. Earthscan; 2009.

[14] Chang TJ, Wu YT, Hsu HY, Chu CR, Liao CM. Assessment of wind characteristics and wind turbine characteristics in taiwan. Renewable Energy 2003;28(6):851–71.

[15] International Electrotechnical Commission (IEC) . IEC TS 61400-26-2 Ed. 1, Wind turbines - part 26-2: production-based availability for wind turbines. IEC; 2014.

[16] Xia Y, Ahmed KH, Williams BW. Wind turbine power coefficient analysis of a new maximum power point tracking technique. IEEE Transactions on Industrial Electronics 2013;60(3):1122–32.

[17] Kjellin J, Bülow F, Eriksson S, Deglaire P, Leijon M, Bernhoff H. Power coefficient measurement on a 12 kw straight bladed vertical axis wind turbine. Renewable Energy 2011;36(11):3050–3.

[18] Bianchi FD, Battista Hd, Mantz RJ. Wind turbine control systems. Springer-Verlag London; 2007.

[19] Jiang Z, Karimirad M, Moan T. Dynamic response analysis of wind turbines under blade pitch system fault, grid loss, and shutdown events. Wind Energy 2014;17(9):1385–409.

[20] Qiao W, Lu D. A survey on wind turbine condition monitoring and fault diagnosis—part i: Components and subsystems. IEEE Transactions on Industrial Electronics 2015;62(10):6536–45.

[21] Shokrzadeh S, Jozani MJ, Bibeau E. Wind turbine power curve modeling using advanced parametric and nonparametric methods. IEEE Transactions on Sustainable Energy 2014;5(4):1262–9.

[22] González-Longatt F, Wall P, Terzija V. Wake effect in wind farm performance: steady-state and dynamic behavior. Renewable Energy 2012;39(1):329–38.

[23] McKay P, Carriveau R, Ting DSK. Wake impacts on downstream wind turbine performance and yaw alignment. Wind Energy 2013;16(2):221–34.

[24] Gebraad PMO, Teeuwisse FW, Wingerden JW, Fleming PA, Ruben SD, Marden JR, et al. Wind plant power optimization through yaw control using a parametric model for wake effects—a CFD simulation study. Wind Energy 2016;19(1):95–114.

[25] Kusiak A, Song Z. Design of wind farm layout for maximum wind energy capture. Renewable Energy 2010;35(3):685–94.

[26] Emami A, Noghreh P. New approach on optimization in placement of wind turbines within wind farm by genetic algorithms. Renewable Energy 2010;35(7):1559–64.

[27] Porté-Agel F, Wu YT, Lu H, Conzemius RJ. Large-eddy simulation of atmospheric boundary layer flow through wind turbines and wind farms. Journal of Wind Engineering and Industrial Aerodynamics 2011;99(4):154–68.

[28] Barthelmie RJ, Jensen LE. Evaluation of wind farm efficiency and wind turbine wakes at the nysted offshore wind farm. Wind Energy 2010;13(6):573–86.

[29] Barthelmie RJ, Frandsen ST, Nielsen M, Pryor S, Rethore PE, Jørgensen HE. Modelling and measurements of power losses and turbulence intensity in wind turbine wakes at middelgrunden offshore wind farm. Wind Energy 2007;10(6):517–28.

[30] Esteban MD, Diez JJ, López JS, Negro V. Why offshore wind energy? Renewable Energy 2011;36(2):444–50.